Morphological and Broadband Dielectric Spectroscopy Approaches on PA6 - CNT Nanofibres

MONICA ALINA CALIN[1], NABYL KHENOUSSI[2], LAURENCE SCHACHER[2], DOMINIQUE ADOLPHE[2], LILIANA ROSEMARIE MANEA[1]*, IRINA GRADINARU[3], IRINA ZETU[3], SORIN STRATULAT[3]

[1] Technical „Gheorghe Asachi" University of Iasi, Faculty of Textile-Leather Engineering and Industrial Management, 67 D. Mangeron Blv., 700050, Romania

[2] Laboratoire de Physique et Mécanique Textiles EAC 7189 CNRS/UHA,ENSISA, 11 rue Alfred Werner F-68093 Mulhouse Cedex France

[3] „Gr. T. Popa" University of Medicine and Pharmacy of Iasi, Faculty of Dental Medicine, 16 Universitatii Str., 700115, Iasi, Romania

The wide band dielectric spectroscopy analysis of the 1.5% multi walled carbon nanotube (MWNT) contain and 20% polyamide 6 (PA6) nanowebs obtained by three different treatments applied to the MWNTs (chemical, mechanical and mixed) was investigated. A morphological analysis of the samples was carried out using the scanning electron microscopy (SEM) and atomic force microscopy (AFM) principles. The evolution of the dielectric constant (Eps'), imaginary permittivity (Eps"), dissipation factor (Tan δ) and the conductivity modulus were analysed, both from an experimental and a theoretical point of view.

Keywords: nanowebs, polyamide 6, multi walled carbon nanotubes, wide band dielectric spectroscopy

Nanofibers have a large variety of applications in many fields. In the medical field, nanofibers can be used as tissue engineering scaffolding: porous membranes for skin, tubular shapes for blood vessels and nerve regenerations, three-dimensional (3D) scaffolds for bones and cartilage regenerations; they can have a cosmetic use as skin cleansers, skin healing, skin therapy with medicine [1,2]. Nanofibers play an important role in the filter industry for liquid, gas or molecule filtration, they are also used in military protective clothing due to their minimal impedance to air, efficiency in trapping aerosol particles, or their anti-bio-chemical gases behaviour. Nanofibers can be excellent nanosensors: thermal, piezoelectric, biochemical, fluorescence optical sensors, etc., or they can have other industrial applications such as: micro/nano electronic devices, electrostatic dissipation, electromagnetic interference shielding, photovoltaic devices, LCD devices, ultra-lightweight spacecraft materials, etc. [3].

The most common method of obtaining nanofibers is the electro-spinning process. The electrospinning principle consists in the formation of the nanofibers by expelling a jet of polymeric solution or melt through a spinneret under high voltage. The applied voltage helps the formation of the Taylor cone at the tip of the needle and of the electrospinning jet [4]. On the way from the tip of the spinneret to the collecting area, the solvent evaporates, the jet solidifies resulting the nanofibers. The distance between the tip of the needle and the collecting area allows the solvent (formic acid) to dissolve and helps the formation of the nanofibers [5]. The process also needs two electrodes: one to be in contact with the spinneret and the other one to be in contact with the collecting area. For the solution spinning, it is required to use solvents to dissolve the polymers and create the electrospinning solution. Usually, both the dissolving of the polymers and the electrospinning process take place at the room temperature and normal atmospheric conditions [6, 7].

In this study there were obtained polymeric nanofibers reinforced with different concentrations of CNT: 0,5, 1, 1,5 and 2%. The concentration of the polymer for all solutions was 10% PA6. In order to obtain the electrospinning solutions, three different treatments were applied to the CNT: chemical treatment, mechanical treatment and mixed treatment (chemical and mechanical). The modulus conductivity of the obtained samples was analysed by studying the dielectric spectroscopy. The experimental behaviour of the conductivity modulus was mathematically explained.

Experimental part

Materials

The materials used in order to obtain the nanowebs were: polyamide 6 (PA6); multi-wall carbon nanotubes (MWNT), from Arkema Company, France; sulphuric acid (H_2SO_4) of 50% purity, nitric acid (HNO_3)of 65% purity and formic acid (CH_2O_2) of 90% purity from Fisher Scientific Company, France.

The sulphuric acid and nitric acid were used for the chemical and mechanical treatment applied to the MWNTs. Formic acid was used in order to dissolve the polymer, PA6, which was purchased as pellets of 3mm medium size, from Sigma-Aldrich (France).

In the preliminary stage, three different types of treatments were applied to the MWNTs: chemical, mechanical and mixed. For each of the three treatments, a 1.5% MWNT-20%PA6 electrospinning solution was prepared as follows.

Chemical treatment

A 65% HNO_3 and 50% H_2SO_4 (v/v=1:3) acid solution was prepared in an Erlenmeyer glass and 2g of MWNTs were added. The mixture was left to sonication at 50°C for 4 h (30 min sonication and 5 min pause). Next, the MWNTs were separated from the mixture of acids and washed

* *Tel.: (+40) 0232 278683*

with oxygenated water in order to obtain a *p*H=7 of the residual water. The MWNTs were dried in an oven at 130°C, for 48 h . The equivalent of the 1.5% MWNTs concentration was dispersed into 27.77ml of CH_2O_2, 90% purity (the equivalent of 25mL of pure CH_2O_2) together with the PA-6 pellets, equivalent to a 20% concentration. The mixture was left on a magnetic stirrer for 72 h at 70°C, in order to facilitate the dissolving process of the PA-6 and homogenize the solution.

The solution was left to reach the room temperature before being electrospun [8].

Mechanical treatment

For the mechanical treatment, 0.5828g, of MWNTs corresponding to the 1.5% concentration was dispersed into 27.77mL of CH_2O_2 (90% purity) and left for 1 h at sonication, at 50°C. Next, the solution was mixed with the Ika® T25digital Ultra Turrax®, at 18.000rpm for 30 min. Then, the PA-6 pellets were added and the solution was left for 72 h at 70°C on a magnetic stirrer. It resulted a mechanically treated solution which was left to reach the room temperature [8].

Mixed treatment

The mixed treatment consists of a combination of the chemical and mechanical treatments, applied to the MWNTs. First, the v/v=1:3 mixture of 65% HNO_3 and 50% H_2SO_4 was prepared in order to chemically treat 2g of MWNTs. The solution was put to sonication at 50°C for 4 h. After that, it was mixed with the Ultra Turrax equipment at 18.000 rpm for 30 min. Next, the treated MWNTs were separated from the acidic mixture and were put to a washing procedure with oxygenated water in order to obtain the *p*H=7 of the residual water. After that, the MWNTs were dried in an oven at 130°C, for 48 h. A quantity corresponding to a 1.5% MWNT concentration was dispersed into 27.77 mL of 90% CH_2O_2 together with the PA-6 pellets, equivalent of the 20% concentration. The resulted solution was left for 72 h at 70°C on a magnetic stirrer. After that it was left to reach the room temperature for the electrospinning process [8].

Electrospinning conditions

The experimental electrospinning device used was built in the "Laboratoire de physique et Mécanique Textiles", ENSISA - Mulhouse (France) [9]. The 3 solution were electrospun for 15 min each for the morphological analysis and 60 min each, for the wide band dielectric spectroscopy analysis, using the following parameters:

- 0.7x30mm needle;
- 15cm distance from the needle to the collecting area;
- 0.283mL feed rate;
- 20 mL syringe;
- 30kV voltage;
- room temperature conditions: 30% humidity and 20°C.

The applied voltage helped the formation of the Taylor cone at the tip of the needle, and the formation of the electrospinning jet [6, 7, 10]. The 15 cm distance between the tip of the needle and the collecting area allows the formic acid to dissolve in order to obtain the nanofibers. For the morphological analysis the collecting surface was made from copper, covered by an aluminium foil while for the wide band dielectric spectroscopy analysis the collecting surface was made of teflon.

Results and discussions

Morphological analysis

From each of the samples electrospun on aluminium foil, 3 specimens were taken in order to be studied with the scanning electron microscope (SEM), as shown in the picture below:

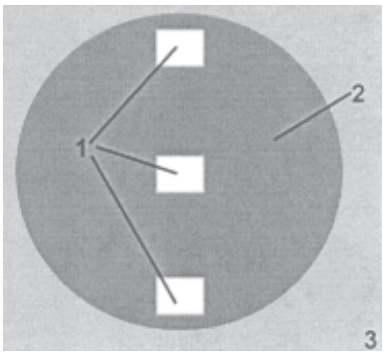

Fig. 1. Electrospun sample 1-specimens; 2-sample resulted after electrospinning; 3-copper surface covered by an aluminium foil

Table 1
PA6-MWNT NANOFIBERS DIAMETERS

Type	Specimen	Position	Statistical values		
			Average (nm)	SD	C_v %
CHEMICAL	1.1	upper ext.	129.33	40.2	31.08
	1.2	center	136.26	40.3	29.58
	1.3	bottom ext.	155.92	28.82	18.48
	Sample 1		140.5		
MECHANICAL	2.1	upper ext.	113.52	15.11	13.31
	2.2	center	102.49	22.15	21.61
	2.3	bottom ext.	100.77	18.25	18.11
	Sample 2		105.59		
MIXED	3.1	upper ext.	95.93	30	31.27
	3.2	center	99.21	28.09	28.31
	3.3	bottom ext.	80.95	8.87	10.96
	Sample 3		92.03		

The specimens were analysed with the Hitachi S-230N SEM, from „Laboratoire de Physique et Mécanique Textiles", ENSISA – Mulhouse (France), in order to study the homogeneity of the nanofibers and to determine their diameters. The SEM analysis of the PA6-CNT nanofibers required a preliminary coating step of the samples, in order to achieve good quality images. The samples were coated with a thin gold layer using the Elexience coating device. The conductive layer of gold scatters the electrons, preventing the accumulation of charge on the sample surface, thus helping to improve image contrast.

For each of the specimens, there were taken pictures at different levels of magnification: x800, x5K and x10K. On the x10K level of magnification, the diameters of 100 nanofibers per sample were measured and the average diameter, standard deviation and variation coefficient were calculated. The values obtained are summarized in table 1.

According to the obtained results, it can be easily observed that the values of the average diameters varied between 80.95nm for the mixed treatment and 155.92nm for the chemical treatment. As it can be seen also on the SEM pictures, the chemical treatment resulted in thicker but more homogenous nanofibers, with the few defects (few beads and solvent traces), while the mixed treatment gave the thinnest diameters of the nanofibers, but with a lot of defects of the surface (large number of beads, flat nanofibers). On the mechanical treatment, the number of beads is bigger than on the chemical treatment, but is considerably smaller than for the mixed treatment (table 2) [11-13].

Table 2
SEM IMAGES OF THE PA6-CNT NANOFIBERS

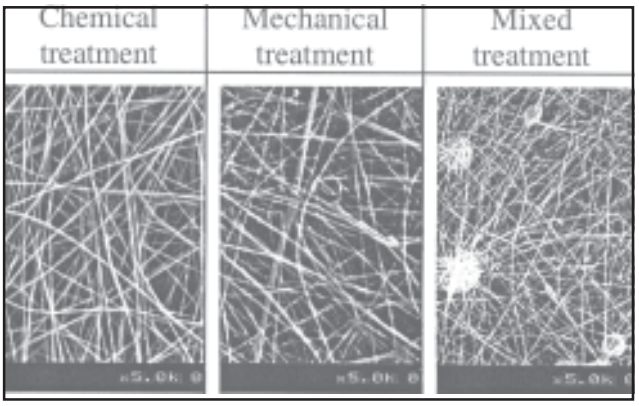

The atomic force microscopy (AFM) was used in order to investigate the surface roughness of the PA6-MWNT nanowebs. The analysis was performed at the „Institute of Macromolecular Chemistry", Petru Poni – Iasi on the NTEGRA Spectra NT-MDT microscope. The roughness values of about 50 nanofibers per sample were analysed using the Gwyddion software. Gwyddion is a free modular application for SPM (scanning probe microscopy) data visualization and analysis. Primarily it was intended for analysis of height fields obtained by scanning probe microscopy techniques (AFM, MFM, STM, SNOM/NSOM), however it can be generally used for any other height field and image analysis, for instance for analysis of profilometry data. The topographic images obtained can be observed in table 4. The average values of the Roughness average (Ra) and the Average maximum height of the profile (Rz) were obtained (table 3) [14].

Table 3
AVERAGE ROUGHNESS VALUES OF THE PA6-CNT NANOFIBERS

	Chemical treatment	Mechanical treatment	Mixed treatment
Ra(nm)	7	2.24	4.68
Rz(nm)	32.6	13.42	17.44

Some roughness graphs corresponding to each of the applied treatments are presented in figure 2.

The SEM results regarding the homogeneity of the nanofibers are also confirmed by the AFM analysis: the nanowebs obtained by the chemical treatment are the most homogenous, opposite to the ones obtained by the mixed treatment [14].

Wide band dielectric spectroscopy analysis

Protocol of work

The dielectric properties of the samples were analysed by studying the broadband dielectric spectroscopy, with a Novocontrol GmbH broadband dielectric spectrometer, Germany. Based on the interactions between the electromagnetic field and matter, the broadband dielectric spectroscopy can determine the dielectric parameters in a wide frequency range (10^{-6}Hz – 3GHz), at temperature values between -160°C and 400°C [15]. For the measurements of the samples, an RF sample cell was used and the dimension of the plan-parallel electrods was of 5mm diameter.

The protocol of work was made of the following steps:

- calibration of the extension line;

Table 4
SURFACE TOPOGRAPHY OF PA6-CNT NANOFIBERS

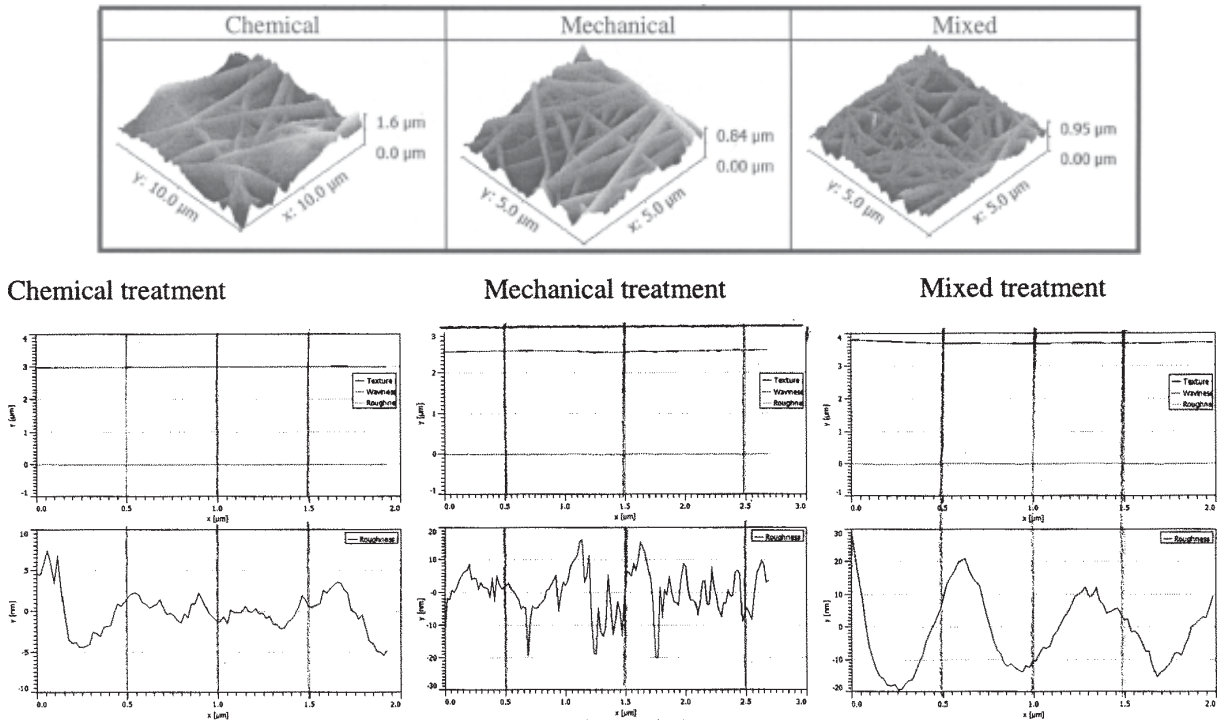

Fig. 2. Roghness graphs

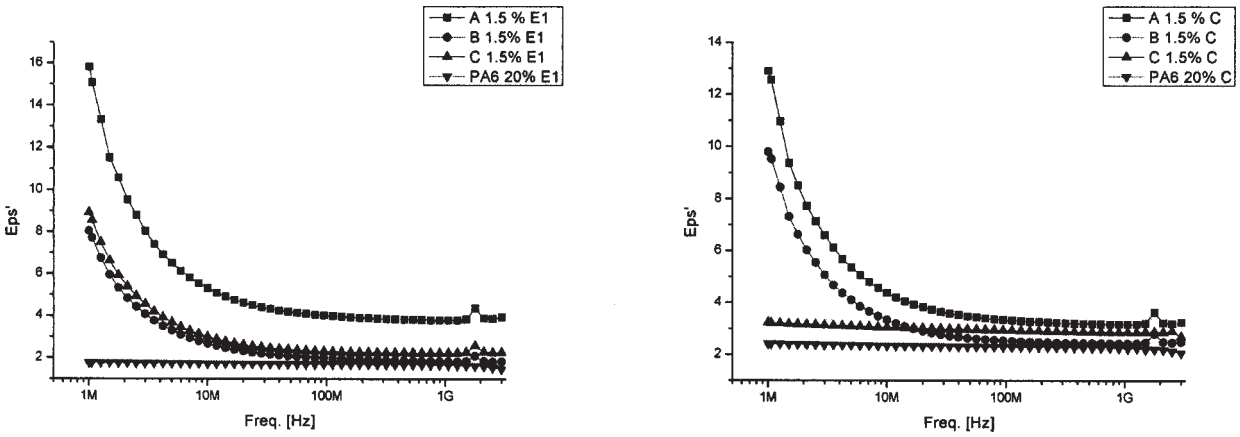

Fig. 3. The evolution of the Eps'- exterior vs. central samples

- calibration of the sample cell (both in open and closed circuit);

- sample measurements, under ambient conditions at a frequency interval of 10^{-6}Hz and 3GHz frecquency.

Two specimens (one in exterior and one in the center) for each of the three samples were analysed and compared to a pristine, 20% polyamide 6 sample. The influence of the carbon nanotubes and of the treatment applied to them was investigated.

The evolution of the dielectric constant – Eps'

Analysing the evolution of the dielectric constant of the samples, an increasing behaviour for the central samples can be observed. This can be explained by the fact that in the centre, the samples present a greater capacity of storing energy comparing to the exterior (on the exterior samples, the dielectric constant is decreasing - fig. 3). A significant increase of the values of the dielectric constant can be observed for lower frequencies. This behaviour is due to the increasing number of interferences between the polymeric matrix and the CNTs [16-19].

Regarding the treatments applied to the CNTs, it can be observed that the dielectric constant increases for the chemically treated samples. For the mechanical and mixed treatments the dielectric constant is decreasing (fig. 3).

Regarding the samples' ability to store energy relative to the treatments applied to the CNTs, it can be concluded that the values and the evolution of the dielectric constant are not significantly influenced by the applied treatments. The mechanical and the mixed treatments have low values for the dielectric constant; the chemical treatment does not cause additional dielectric polarizations. This behaviour shows that the dielectric constant is not significantly affected by the CNT contain of the analysed nanofibers.

It can be concluded that the dielectric constant Eps' increases with the mobility. More than that, a high mobility decreases the interactions between the PA6 and the CNTs.

The evolution of the imaginary permittivity – Eps"

The dielectric losses decrease with the increase of the frequency. For frequency values close to 1 MHz, appears the interfacial polarization. The polarization is caused by the dielectric charge carriers which have enough time to move both at the interface of the polymeric matrix and CNTs and at the contact surface between the measurement electrodes and the analysed sample. Basically, the dielectric charges move between the interface of the CNT and the basic matrix (PA6), causing the increase of the total polarization.

The treatments applied to the CNTs lead to an increase of the imaginary permittivity related to the CNT contain. The chemical treatment does not influence the dielectric properties of the nanofibers. The spectral evolution confirms the existence of an interfacial polarization phenomenon. PA-6 has a neutral behaviour in dielectric terms. The non-polar character of the PA-6 sample turns into a highly polar one, with the addition of the CNTs (fig. 4).

The interactions between the PA-6 and the CNTs increase together with the increasing of the values of the imaginary permittivity Eps".

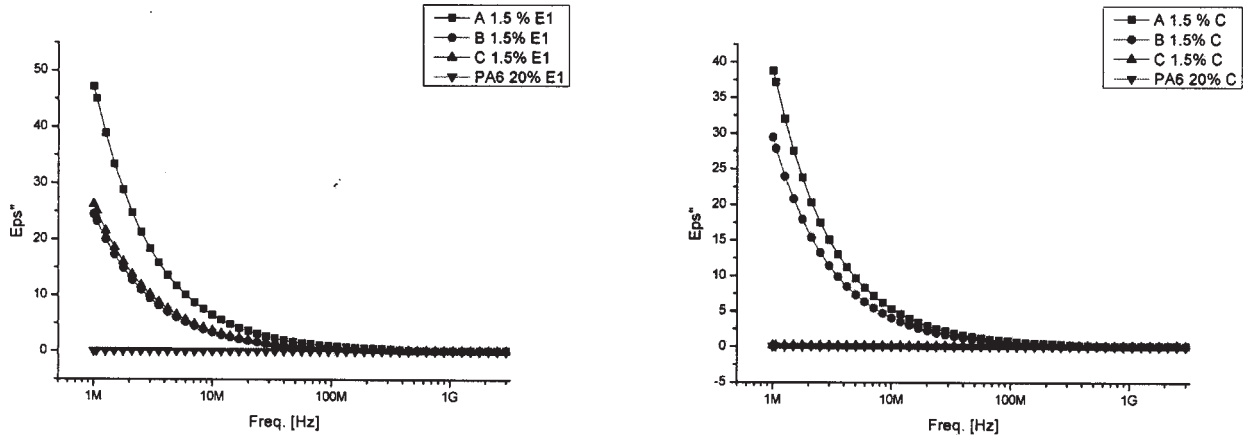

Fig. 4. The evolution of the Eps"- exterior vs. central samples A – chemical treatment; B – mechanical treatment; C- mixed treatment

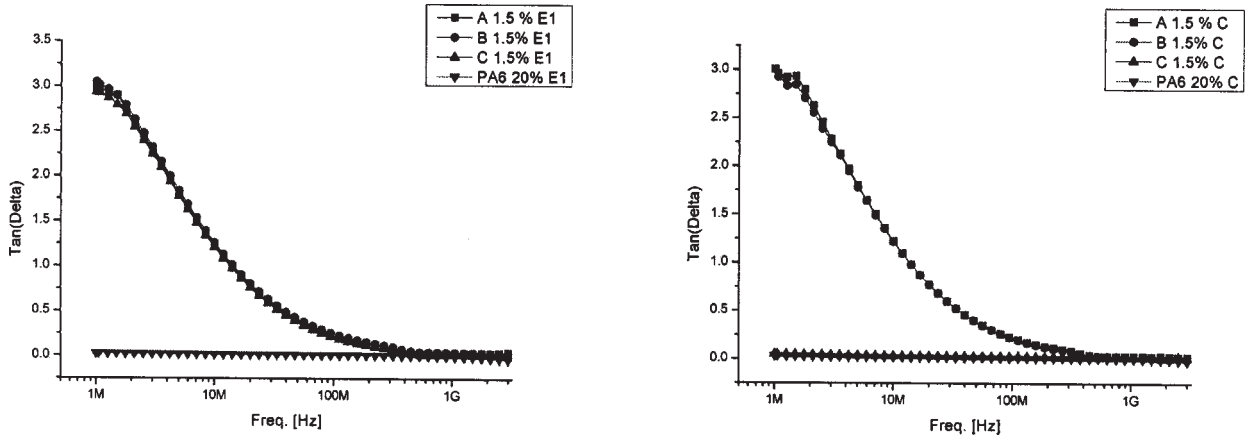

Fig. 5. The evolution of the Tan (δ)- exterior vs. central samples A – chemical treatment; B – mechanical treatment; C- mixed treatment

The evolution of the dissipation factor – Tan (δ)

A dielectric relaxation for the chemical and mechanically treated samples can be observed, phenomenon which is not present for the standard PA6 sample. For the low frequencies, dielectric relaxations and increasing dielectric dissipations occur. The dielectric , properties of the nanofibers are not influenced by the treatments applied to the CNTs.

Regarding the position of the analysed samples (central or exterior, no difference between the values of the dissipations can be observed - fig. 3).

Mathematical model

Due to the fact that Debye's model does not describe the behaviour of the composite (CNT-PA6), which can be observed for the majority of the compounds having PA6 matrix, the model was generalized by including some processes characterized through a series of relaxation times. By choosing a distribution for the relaxation periods, the response of the composite can be well configured [20]. This way, by using the distribution model of the relaxation times, one can explain the origin of the constant phase elements which are used to study the solid-solid interfaces. It must be mentioned that recently, the universal response model is being used as an alternative to the distribution model of the relation times [21, 22].

The superposition principle allows the generalization of the relative permittivity formulae, as follows

$$\varepsilon_{(\omega)} = \varepsilon_{(\omega)}^{'} - i\varepsilon^{''}(\omega) = \varepsilon_{\infty} + \int_0^{\infty} \frac{(\varepsilon_s - \varepsilon_{\infty})G(\tau)d\tau}{1+i\omega\tau} \quad (1)$$

where G(τ) is the distribution function of the relaxation times. The distribution satisfies the normalization condition

$$\int_0^{\infty} G(\tau)d\tau = 1 \quad (2)$$

where G(τ) is the ratio from the total dispersion (ε_s - ε_∞), determined by processes which have the relaxation time between τ and τ + dτ. In equation (1), ε_s is the relative electric permittivity for ω = 0, while ε_∞ is the relative electric permittivity for $\omega \to \infty$.

If in equation (1) we separate the real part from the imaginary part, it can be found that:

$$\varepsilon_{(\omega)}^{'} = \varepsilon_{\infty} + \int_0^{\infty} \frac{G(\tau)(\varepsilon_s - \varepsilon_{\infty})}{1+(\omega\tau)^2} d\tau \quad (3)$$

$$\varepsilon_{(\omega)}^{''} = \int_0^{\infty} \frac{\omega\tau G(\tau)(\varepsilon_s - \varepsilon_{\infty})}{1+(\omega\tau)^2} d\tau \quad (4)$$

One of the most used distributions is the one proposed by Cole [23, 24]. The behaviour of the relative permittivity is described by the equation below [8]:

$$\varepsilon_{(\omega)} = \varepsilon_{\infty} + \frac{\varepsilon_s - \varepsilon_{\infty}}{1+(i\omega\tau)^{1-\alpha}} \quad (5)$$

where α is a parameter which is dependent of the relaxation processes, with $0 \le \alpha < 1$. For α=0, equation (5) can be reduced to Debye's equation:

$$\varepsilon_{(\omega)} = \varepsilon_{\infty} + \frac{\varepsilon_s - \varepsilon_{\infty}}{1+i\omega\tau} \quad (6)$$

which highlights the following dependencies:

$$\varepsilon_{(\omega)}^{'} = \varepsilon_{\infty} + \frac{\varepsilon_s - \varepsilon_{\infty}}{1+(\omega\tau)^2} \quad (7)$$

$$\varepsilon_{(\omega)}^{''} = \frac{(\varepsilon_s - \varepsilon_{\infty})\omega^2}{1+(\omega\tau)^2} \quad (8)$$

The general situation (5), leads to the following dependencies:

$$\varepsilon_{(\omega)}^{'} = \varepsilon_{\infty} + \frac{(\varepsilon_s - \varepsilon_{\infty})\left\{1+(\omega\tau)^{1-\alpha}\cos\left[\frac{\pi}{2}(1-\alpha)+2k\pi(1-\alpha)\right]\right\}}{1+(\omega\tau)^{2(1-\alpha)}+2(\omega\tau)^{1-\alpha}\cos\left[\frac{\pi}{2}(1-\alpha)+2k\pi(1-\alpha)\right]} \quad (9)$$

$$\varepsilon_{(\omega)}^{''} = \frac{(\varepsilon_s - \varepsilon_{\infty})(\omega\tau)^{1-\alpha}\sin\left[\frac{\pi}{2}(1-\alpha)+2k\pi(1-\alpha)\right]}{1+(\omega\tau)^{2(1-\alpha)}+2(\omega\tau)^{1-\alpha}\cos\left[\frac{\pi}{2}(1-\alpha)+2k\pi(1-\alpha)\right]} \quad (10,11)$$

$$k = 0,1...\alpha/\alpha - 1$$

The dependencies (7) and (8) are presented below, fig. 6 a,b and 7 a,b.

The theoretical dependencies from the fig. 6a,b and 7a,b describe only qualitatively our experimental results, through the asymptotic areas of the curves. However, the "functionalities" of the theoretical model relative to our experimental results, can be obtained through an additional hypothesis, one of the dependency

$$\varepsilon_s = \varepsilon_s(r) \quad (12)$$

where ρ is the density of the composite. Due to the fact that ε_s increases together with the density, the curves from figure 8 a,b and 9 a,b can be obtained

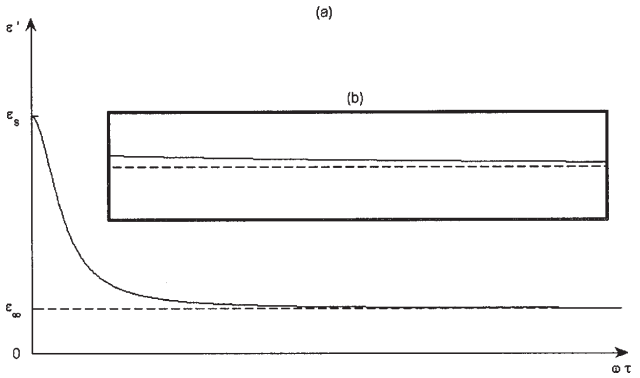

Fig. 6. The dependency of the real part of the relative electric permittivity on ωτ (a); Zoom in of the same dependency, associated to the asymptotic "regime" (b)

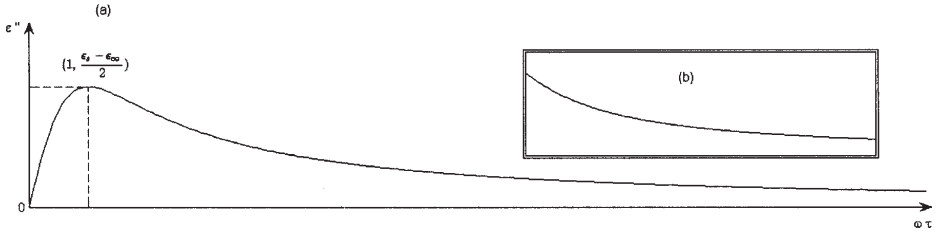

Fig. 7. The dependency of the imaginary part of the relative electric permittivity on ωτ (a); Zoom in of the same dependency, associated to the asymptotic "regime" (b)

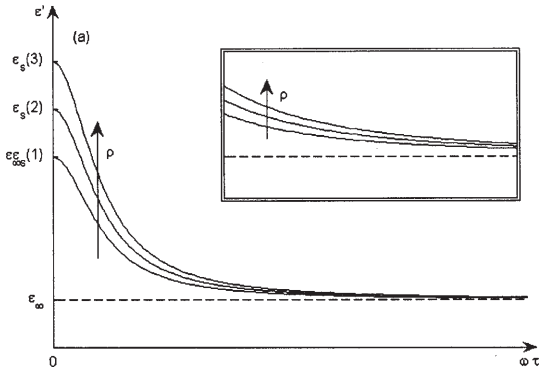

Fig. .8. The dependencies of the real part of the relative electric permittivity, on ωτ for different densities (a); Zoom in for the same dependency, associated to the asymptotic "regime" for different densities (b)

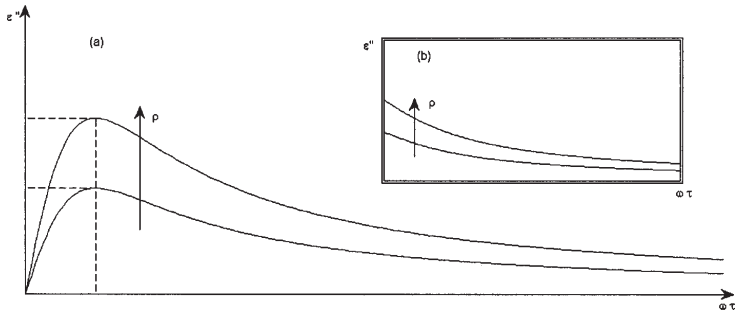

Fig. 9. the dependencies of the imaginary part of the relative electric permittivity, on ωτ for different densities (a); Zoom in for the same dependency, associated to the asymptotic "regime" for different densities (b)

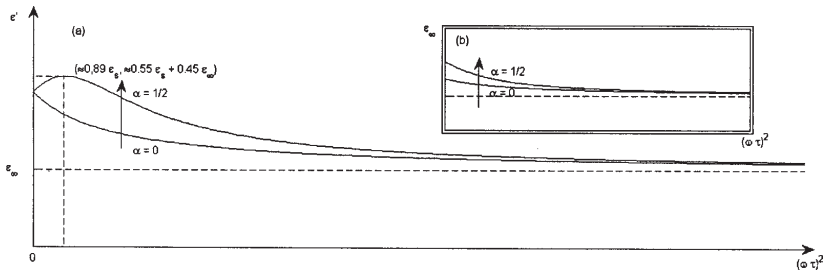

Fig. 10. The dependencies of the real part of the relative electric permittivity, for different densities, on $(\omega\tau)^2$, for $\alpha=0$ and $\alpha=1/2$ respectively (a); Zoom in for the same dependency, associated to the asymptotic "regime", for $\alpha=0$ and $\alpha=1/2$ respectively (b)

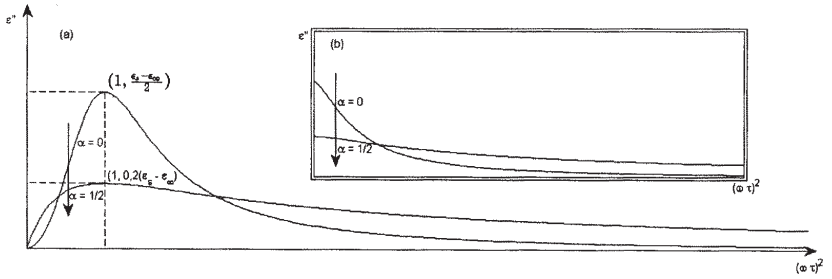

Fig. 11 The dependencies of the imaginary part of the relative electric permittivity, for different densities, on $(\omega\tau)^2$, for $\alpha=0$ and $\alpha=1/2$ respectively (a); Zoom in for the same dependency, associated to the asymptotic "regime", for $\alpha=0$ and $\alpha=1/2$ respectively (b)

We can exclude hypothesis (12), admitting the "functionalities" of the equations (9) and (10). In this situation, for $\alpha=1/2$ and k=0, the following equations are obtained:

$$\varepsilon' = \varepsilon_\infty + \frac{(\varepsilon_s - \varepsilon_\infty)\left(1+\sqrt{\frac{\omega\tau}{2}}\right)}{1+(\omega\tau) \ +\sqrt{2\omega\tau}} \qquad (13)$$

$$\varepsilon'' = \frac{(\varepsilon_s - \varepsilon_\infty)\sqrt{\frac{\omega\tau}{2}}}{1+\omega\tau+\sqrt{2\omega\tau}} \quad (14)$$

Figures 10a,b and 11a,b present the (13) and (14) dependencies.

The fact that the second alternative generated through the equations (13) and (14) allows a good interpretation of the experimental results, specifies a fractal mechanism for the relaxation of the composite, through the power type general equations ((9) ; (10)). It is known that the multi-scale systems type (which have more relaxation times), the functional dependencies between the physical quantities which describe the dynamics of the physical system, are fractal.

Conclusions

The main conclusions of the present paper are the following:

- the conductivity modulus of polyamide 6 (PA6) – carbon nanotubes (CNT)
- nanowebs, obtained by electrospinning process is studied;
- the influence of both the applied treatment and the CNT contain was investigated by analysing the broadband dielectric spectroscopy of the samples;
- a theoretical model is established in order to explain the dynamics of the electric conductivity in PA6-CNT nanowebs;
- our experimental results are well described by the theoretical model. A fractal type mechanism is established given the multiplicity of the relaxation times.

References

1. LEE, K.Y., JEONG, L., KANG, Y.O., LEE, S.J., PARK, W.H., Adv. Drug Deliv. Rev., **61**, nr. 12, 2009, p. 1020
2. CALIN, M.A., et al., Textile industry at nanoscale, 14th Romanian Textiles and Leather Conference – CORTEP 2012, Sinaia, Romania, 6-8 September, 2012
3. Huang, Z. M., ZHANG, Y.Z., KOTAKI, M., Compos. Sci. Technol., **63**, 2003, p. 2223
4. PHAM, Q.P., SHARMA, U., Mikos, A.G., Tissue Eng., **12**, nr. 5, 2006, p.1197
5. SUBBIAH, T., BHAT, G.S., PARARNESWARAN, S., RAMKUMAR S.S., J. Appl. Polym. Sci., **96,** nr. 2, 2005, p.557
6. RAMAKRISHMA, S., An introduction to electrospinning and nanofibers, World Scientific Publishing Co. Pre., Singapore, 2005, ISBN 981-256-415-2
7. DOSHI, J., RENEKER, D.H., J. Electrost., **35**, nr. 2-3, 1995, p.151
8. CALIN, M.A., Nanofibre senzoriale pe baza de nanotuburi de carbon, Ed. Ars Longa, Iasi, 2013, ISBN 978-973-148-130-2
9. KHENOUSSI, N., SCHACHER, L., ADOLPHE, D., Exp. Tech., **36**, nr. 2, 2012, p. 32
10. CALIN, M.A., et al., Characterization of MWNT-reinforced PA6 nanocomposites (produced by electrospinning), 12th World Conference Autex 2012, Zadar, Croatia,13-15 June, 2012
11. CALIN, M.A., MWNT – Reinforced PA6 Nanocomposites Obtained by Electrospinning, (E U R O I N V E N T - European Exhibition of Creativity and Innovation - Iasi, Romania, 10-12 May, 2012
12. CALIN, M.A., et al., Determination of the optimum electrospinning parameters of a MWNT-reinforced PA6 solution, I N V E N T I C A 2012 - Iasi, Romania, 13-15 June, 2012
13. CALIN, M.A., et al., Homogenous MWNT-reinforced PA6 nanofibers obtained by electrospinning, I N V E N T I C A 2012 - Iasi, Romania, 13-15 June, 2012
14. CALIN, M.A., CURTEZA, A., TOMA, S., AGOP, M., Metal. Int., **18**, nr. 1, 2013, p. 19
15. CALIN, M.A., CURTEZA, A., KHENOUSSI, N., et al., Metal. Int., **18**, nr. 1, 2013, p. 23
16. MUNCELEANU, G.V., PAUN, V.P., CASIAN-BOTEZ, I., AGOP, M., Int. J. Bifurcation Chaos, **21**, nr. 2, 2011, p. 603
17. CASIAN-BOTEZ, I., AGOP., M., NICA, P.E., PAUN, V.P., MUNCELEANU, G.V., J. Comput. Theor. Nanosci., **7**, nr. 11, 2010, p. 2271
18. BORSOS, Z., PĂUN, V.P., CASIAN-BOTEZ, I., STOICA, C.M., VIZUREANU, P., AGOP, M., Rev. Chim.(Bucharest), **59**, no. 10, 2008, p. 1169
19. AGOP, M., PAUN, V., HARABAGIU, V., Chaos Solitons Fractals, **37**, nr. 5, 2008, p. 1269
20. AGOP., M., NICA, P.E., IOANNOU, P.D., ANTICI, A., PĂUN, V.P., Eur. Phys. J. D, **49**, nr. 2, 2008, p. 239
21. PAUN, V.P., Mat. Plast., **44**, no. 4, 2007, p. 393
22. VIZUREANU, P., AGOP, M., Mater. Trans., 2007, **48**, nr. 11, p. 3021
23. STUERGA, D., Microwave-Material Interactions and Dielectric Properties, Key Ingradients for Mastery of Chemical Microwave Processes, WILEY-VCH Verlag GmbH & Co. KgaA, 2006, ISBN: 3-527-31-452-0
24. CALIN, M.A., et al., Theoretical modelling of a carbon nanotube as temperature sensor, 14th Romanian Textiles and Leather Conference – CORTEP 2012, Sinaia, Romania, 6-8 September, 2012

Manuscript received: 6.07.2013